

Maximization of Extractable Randomness in a Quantum Random-Number Generator

J. Y. Haw,^{1,*} S. M. Assad,¹ A. M. Lance,² N. H. Y. Ng,³ V. Sharma,² P. K. Lam,¹ and T. Symul¹

¹*Centre for Quantum Computation and Communication Technology, Department of Quantum Science,
The Australian National University, Canberra, ACT 0200, Australia*

²*QuintessenceLabs, Unit 1 Lower Ground, 15 Denison Street, Deakin, ACT, 2600 Australia*

³*Centre for Quantum Technologies, National University of Singapore, 3 Science Drive 2, 117543 Singapore*

(Dated: May 20, 2015)

The generation of random numbers via quantum processes is an efficient and reliable method to obtain true indeterministic random numbers that are of vital importance to cryptographic communication and large-scale computer modeling. However, in realistic scenarios, the raw output of a quantum random-number generator is inevitably tainted by classical technical noise. The integrity of the device can be compromised if this noise is tampered with, or even controlled by some malicious party. To safeguard against this, we propose and experimentally demonstrate an approach that produces side-information independent randomness that is quantified by min-entropy conditioned on this classical noise. We present a method for maximizing the conditional min-entropy of the number sequence generated from a given quantum-to-classical-noise ratio. The detected photocurrent in our experiment is shown to have a real-time random-number generation rate of 14 (Mbit/s)/MHz. The spectral response of the detection system shows the potential to deliver more than 70 Gbit/s of random numbers in our experimental setup.

I. INTRODUCTION

Randomness is a vital resource in many information and communications technology applications, such as computer simulations, statistics, gaming, and cryptography. For applications that are not concerned with the security and uniqueness of randomness, a sequence with uniformly distributed numbers mostly suffices. Such sequences can be generated using a pseudorandom-number generator (PRNG) that works via certain deterministic algorithm. Although PRNGs can offer highly unbiased random numbers, they cannot be used for applications that require information security for two reasons: First, PRNG-generated sequences are unpredictable only under limitations of computational power, since PRNGs are inherently based on deterministic algorithms. Second, the random seeds, which are required to define the initial state of a PRNG, limit the amount of entropy in the random-number sequences they generate. This compromises the security of an encryption protocol.

For cryptographic applications [1], a random sequence is required to be truly unpredictable and to have maximum entropy. To achieve this, intensive efforts have been devoted to developing high-speed hardware RNGs that generate randomness via physical noise [2–6]. Hardware RNGs are attractive alternatives because they provide fresh randomness based on physical processes that are apparently unpredictable (i.e. uncorrelated with any existing information either with past settings or side information). Moreover, they also provide a solution to the problem of having insufficient entropy. Because of the deterministic nature of classical physics, however, some of these hardware generators may be only truly

random under practical assumptions that cannot be validated. RNGs that rely on quantum processes (QRNGs), on the other hand, can have guaranteed indeterminism and entropy, since quantum processes are inherently unpredictable [7, 8]. Examples of such processes include quantum phase fluctuations [9–13], spontaneous emission noise [14–16], photon arrival times [17–19], stimulated Raman scattering [20], photon polarization state [21, 22], vacuum fluctuations [23, 24], and even mobile phone cameras [25]. These QRNGs resolve both shortcomings of the PRNGs. However, despite their reliance on entropy which is ultimately guaranteed by the laws of quantum physics, measurements on quantum systems are often tainted by classical noise. We quantify the amount of quantum randomness to the amount of classical noise using a quantum-to-classical-noise ratio (QCNr). When QCNr is low, both the quality and the security of the random sequence generated may be compromised [24, 26, 27].

To address this issue, Gabriel *et al.* [24] took into account potential eavesdropping on the classical noise by considering the channel capacity of their QRNG. Their setup exhibited a good QCNr clearance and was able to extract approximately 3 bits per sample of guaranteed randomness out of 5 bits of digitization (approximately 60%). More recently, Ma *et al.* [26] proposed a framework for QRNG entropy evaluation. By using *min-entropy* as the quantifier for randomness, they extracted a higher rate of random bits of 6.7 bits per sample from 8 bits (approximately 84%), where the quantum contribution of the randomness was obtained by inferring the QCNr.

In the process of generating random bits via measuring continuous-variable systems, an analog-to-digital converter (ADC) is commonly used to discretize the measurement outcomes. It has been speculated [12] that the freedom of choosing the ADC range could be exploited to optimize extractable randomness. Meanwhile,

* jing.yan@anu.edu.au

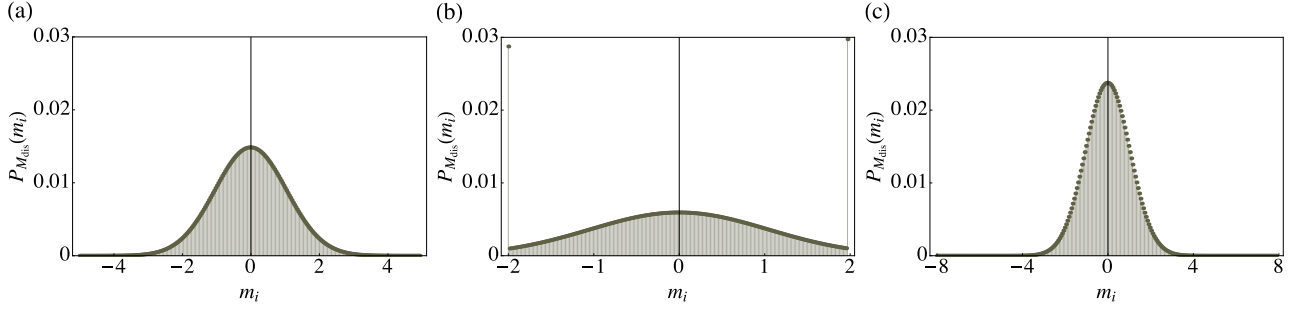


Figure 2. Numerical simulations for the measured distribution probabilities $P_{M_{\text{dis}}}(m_i)$ versus quadrature values, with different dynamical ADC range parameters $R =$ (a) 5, (b) 2 and (c) 8. Without optimization, one will have either an oversaturated or unoccupied ADC bins, which will compromise both the rate and the security of the random-number generation. The parameters used are $n = 8$ and QCNr= 10 dB. The quadrature values are normalized to quantum noise.

i.e. $\text{QCNr} = 10 \log_{10}(\sigma_Q^2/\sigma_E^2)$. The sampling is performed over an n -bit ADC with dynamical ADC range $[-R + \delta/2, R - 3\delta/2]$. Upon measurement, the sampled signal is discretized over 2^n bins with bin width $\delta = R/2^{n-1}$. The range is chosen so that the central bin is centered at zero. The resulting probability distribution of discretized signal M_{dis} reads

$$P_{M_{\text{dis}}}(m_i) = \begin{cases} \int_{-\infty}^{-R+\delta/2} p_M(m) dm, & i = i_{\min}, \\ \int_{m_i-\delta/2}^{m_i+\delta/2} p_M(m) dm, & i_{\min} < i < i_{\max}, \\ \int_{R-3\delta/2}^{\infty} p_M(m) dm, & i = i_{\max}, \end{cases} \quad (2)$$

as shown in Fig. 1 and $m_i = \delta \times i$, where the i are integers $\in \{-2^{n-1}, \dots, 2^{n-1} - 1\}$. The two extreme cases $i = i_{\min}$ and $i = i_{\max}$ are introduced to model the saturation on the first and last bins of an ADC with finite input range, i.e. all the input signals outside $[-R + \delta/2, R - 3\delta/2]$ will be accumulated in the first and last bins. Figure 2 shows the discretized distribution $P_{M_{\text{dis}}}(m_i)$ with different R . We see that an appropriate choice of dynamical ADC range for a given QCNr and digitization resolution n is crucial, since overestimating or underestimating the range will either lead to excessive unused bins or unnecessary saturation at the edges of the bins [28], causing the measurement outcome to be more predictable.

However, in designing a secure CV QRNG, R should not be naively optimized over the measured distribution $P_{M_{\text{dis}}}(m_i)$ but over the distribution conditioned on the classical noise. The conditional PDF between the measured signal M and the classical noise E , $p_{M|E}(m|e)$ is given by

$$p_{M|E}(m|e) = \frac{1}{\sqrt{2\pi(\sigma_M^2 - \sigma_E^2)}} \exp\left[-\frac{(m-e)^2}{2(\sigma_M^2 - \sigma_E^2)}\right] \\ = \frac{1}{\sqrt{2\pi}\sigma_Q} \exp\left[-\frac{(m-e)^2}{2\sigma_Q^2}\right]. \quad (3)$$

This is the PDF of the quantum signal shifted by the classical noise outcome e . By setting $\sigma_Q^2 = 1$, we normalize all the relevant quantities by the quantum noise.

From Eq. (2), the discretized conditional probability distribution is, thus,

$$P_{M_{\text{dis}}|E}(m_i|e) = \begin{cases} \int_{-\infty}^{-R+\delta/2} p_{M|E}(m|e) dm, & i = i_{\min}, \\ \int_{m_i-\delta/2}^{m_i+\delta/2} p_{M|E}(m|e) dm, & i_{\min} < i < i_{\max}, \\ \int_{R-3\delta/2}^{\infty} p_{M|E}(m|e) dm, & i = i_{\max}. \end{cases} \quad (4)$$

With these, we are now ready to discuss how R should be chosen under two different definitions of min-entropy, namely worst-case min-entropy and average min-entropy.

B. Worst-case conditional min-entropy

The min-entropy for variable X with distribution $P_X(x_i)$, in unit of bits, is defined as [35, 38]:

$$H_{\min}(X) = -\log_2 \left[\max_{x_i \in X} P_X(x_i) \right]. \quad (5)$$

Operationally, this corresponds to entropy associated with the maximum guessing probability for an eavesdropper about X . It also tells us about how much (almost) uniform randomness can be extracted out of the distribution $P_X(x_i)$. To obtain a lower bound of the randomness in our entropy source, we first look into the worst-case min-entropy conditioned on classical side information K , which is defined as [39]

$$H_{\min}(X|K) = -\log_2 \left[\max_{k_j \in \text{supp}(P_K)} \max_{x_i \in X} P_{X|K}(x_i|k_j) \right], \quad (6)$$

where the support $\text{supp}(f)$ is the set of values x_i such that $f(x_i) > 0$. In the case of Gaussian distributions, the support of the probability distribution will be \mathbb{R} . Following Eq. (4), upon discretization of the measured signal M , the worst-case min-entropy conditioned on classical

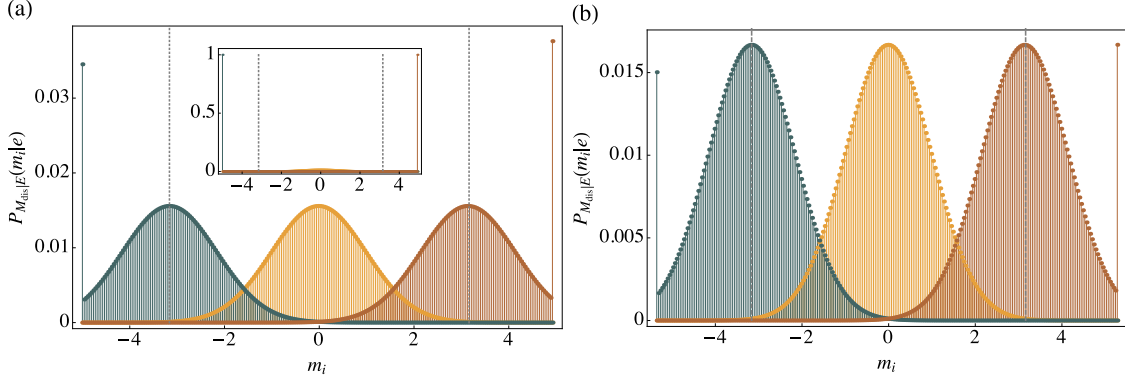


Figure 3. Numerical simulations of: (a) conditional probability distributions $P_{M_{\text{dis}}|E}(m_i|e)$, with $e = \{-10\sigma_E, 0, 10\sigma_E\}$ (from left to right) and $R = 5$. Without optimizing R , when $e = \pm 10\sigma_E$, saturations in the first and last bins affect the maximum of the conditional probability distribution. Inset: $P_{M_{\text{dis}}|E}(m_i|e)$, with $e = \{-100\sigma_E, 0, 100\sigma_E\}$ (from left to right). Unbounded classical noise will lead to zero randomness due to the oversaturation of dynamical ADC. (b) Optimized $P_{M_{\text{dis}}|E}(m_i|e)$, with $e = \{-10\sigma_E, 0, 10\sigma_E\}$ (from left to right). From Eq. (11), the optimal R is chosen to be 5.35. The saturations do not exceed the maximum of the conditional probability distribution whenever $-10\sigma_E \leq e \leq 10\sigma_E$. The parameters are $n = 8$, QCNR = 10 dB. Dashed lines indicate $m_i = \pm 10\sigma_E$. The quadrature values are normalized to vacuum noise.

noise E is

$$H_{\min}(M_{\text{dis}}|E) = -\log_2 \left[\max_{e \in \mathbb{R}} \max_{m_i \in M_{\text{dis}}} P_{M_{\text{dis}}|E}(m_i|e) \right]. \quad (7)$$

Here we assumed that from the eavesdropper's perspective, the classical noise is known fully with arbitrary precision. Performing the integration in Eq. (4), the maximization over M_{dis} in Eq. (7) becomes

$$\begin{aligned} & \max_{m_i \in M_{\text{dis}}} P_{M_{\text{dis}}|E}(m_i|e) \\ &= \max \left\{ \begin{aligned} & \frac{1}{2} \left[1 - \operatorname{erf} \left(\frac{e+R-\delta/2}{\sqrt{2}} \right) \right], \\ & \operatorname{erf} \left(\frac{\delta}{2\sqrt{2}} \right), \\ & \frac{1}{2} \left[\operatorname{erf} \left(\frac{e-R+3\delta/2}{\sqrt{2}} \right) + 1 \right], \end{aligned} \right. \end{aligned} \quad (8)$$

where $\operatorname{erf}(x) = 2/\sqrt{\pi} \int_0^x e^{-t^2} dt$ is the error function. We note that we have $\max_{e \in \mathbb{R}} \max_{m_i \in M_{\text{dis}}} P_{M_{\text{dis}}|E}(m_i|e) = 1$, achieved when $e \rightarrow -\infty$ or $e \rightarrow \infty$. This results in

$H_{\min}(M_{\text{dis}}|E) = 0$ [see inset of Fig. 3 (a)]. Indeed it is intuitive to see that in the case where the classical noise e takes on an extremely large positive value, the outcome of M_{dis} is almost certain to be $m_{i_{\text{max}}}$ with large probability. However, this scenario happens with a very small probability. Hence for practical purposes, one can bound the maximum excursion of e , for example $-5\sigma_E \leq e \leq 5\sigma_E$, which is valid for 99.9999% of the time. With this bound on the classical noise, we now have

$$\begin{aligned} & \max_{e \in [e_{\min}, e_{\max}]} \max_{m_i \in M_{\text{dis}}} P_{M_{\text{dis}}|E}(m_i|e) \\ &= \max \left\{ \begin{aligned} & \frac{1}{2} \left[1 - \operatorname{erf} \left(\frac{e_{\min}+R-\delta/2}{\sqrt{2}} \right) \right], \\ & \operatorname{erf} \left(\frac{\delta}{2\sqrt{2}} \right), \\ & \frac{1}{2} \left[\operatorname{erf} \left(\frac{e_{\max}-R+3\delta/2}{\sqrt{2}} \right) + 1 \right], \end{aligned} \right. \end{aligned} \quad (9)$$

and when $e_{\min} = e_{\max}$,

$$H_{\min}(M_{\text{dis}}|E) = -\log_2 \left[\max \left\{ \frac{1}{2} \left[\operatorname{erf} \left(\frac{e_{\max}-R+3\delta/2}{\sqrt{2}} \right) + 1 \right]; \operatorname{erf} \left(\frac{\delta}{2\sqrt{2}} \right) \right\} \right], \quad (10)$$

which can be optimized by choosing R such that

$$\frac{1}{2} \left[\operatorname{erf} \left(\frac{e_{\max}-R+3\delta/2}{\sqrt{2}} \right) + 1 \right] = \operatorname{erf} \left(\frac{\delta}{2\sqrt{2}} \right). \quad (11)$$

This optimized worst-case min-entropy $H_{\min}(M_{\text{dis}}|E)$ is directly related to the extractable secure bits that are independent of the classical noise. As shown in Fig. 3(a), when Eq. (10) is not optimized with respect to R , the

saturation in the first (last) bin for $e_{\min/\max} = \pm 10\sigma_E$ becomes the peaks of the conditional probability distribution, hence compromising the attainable min-entropy. By choosing the optimal value for R via Eq. (11), as depicted in Fig. 3(b), the peaks at the first and last bins will always be lower than or equal to the probability within the dynamical range. Thus, by allowing the dynamical ADC range to be chosen freely, one can obtain the lowest possible conditional probability distribution, and hence

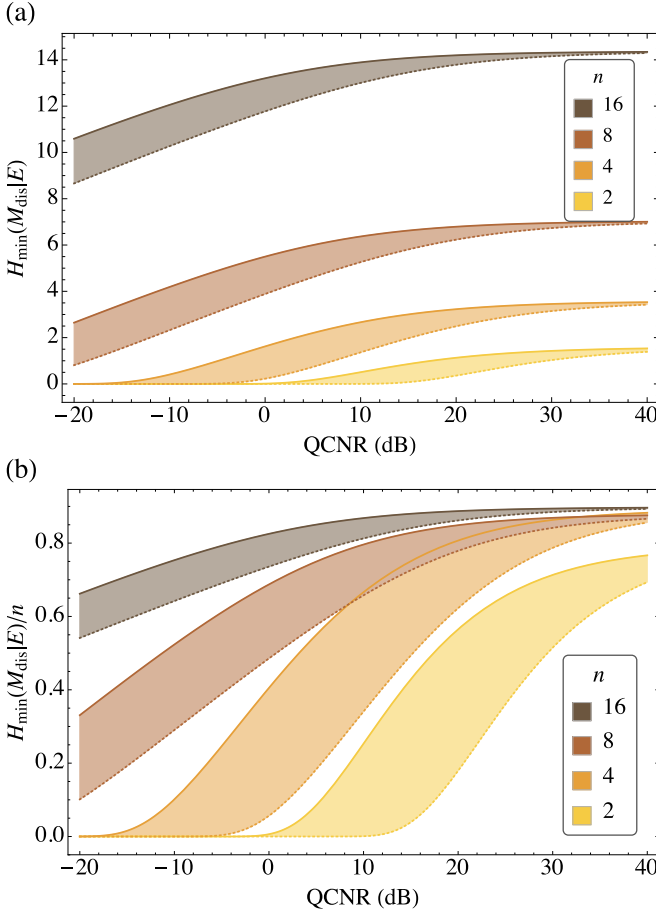


Figure 4. (a) Optimized $H_{\min}(M_{\text{dis}}|E)$ and (b) normalized $H_{\min}(M_{\text{dis}}|E)$ as a function of QCNR for different n -bit ADCs. Shaded areas: $5\sigma_E \leq |e + \Delta| \leq 20\sigma_E$. The extractable bits are robust against the excursion of the classical noise, especially when the QCNR is large. A nonzero amount of secure randomness is extractable even when the classical noise is larger than the quantum noise. The extractable secure randomness per bit increases as the digitization resolution n is increased.

produce the highest possible amount of secure random bits per sample for a given QCNR and n -bit ADC. Equation (10) can be further generalized to take into account the direct current (dc) offset of the device Δ , which can be due to an intrinsic offset of the electronic signal or even a deliberate constant offset induced by the eavesdropper over the sampling period [see Appendix A].

In Fig. 4(a), we show the extractable secure random bits for different digitization n under the confidence interval of $5\sigma_E \leq |e + \Delta| \leq 20\sigma_E$. At the high QCNR regime, the classical noise contribution does not compromise the extractable bits too much. As the classical noise gets more and more comparable to the quantum noise, although more bits have to be discarded, one can still extract a decent amount of secure random bits. More surprisingly, even if the QCNR goes below 0, that is, classical noise becomes larger than quantum noise, in

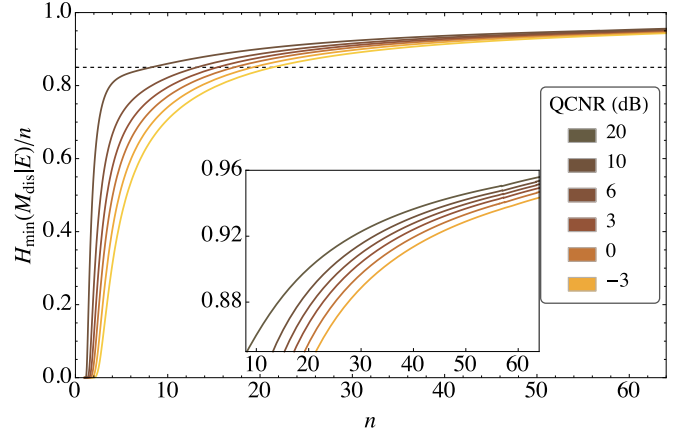


Figure 5. Normalized worst-case conditional min-entropy $H_{\min}(M_{\text{dis}}|E)$ as a function of n -bit ADC for different QCNR values. $|\Delta| = 0$ and $|e| \leq 5\sigma_E$. The interplay between the QCNR and digitization resolution n is shown, where one can improve the rate of secure randomness per bit either by improving the QCNR or increasing n . Inset: Zoom in for $H_{\min}(M_{\text{dis}}|E)/n \geq 0.85$ (dashed line). Even when the classical noise is more dominating compared to the quantum noise (QCNR = -3 dB), 85 % of the randomness per bit can be recovered by having at least approximately 22 bits of digitization.

principle, one can still obtain a nonzero amount of random bits that are independent of classical noise. From Fig. 4(b), we notice the extractable secure randomness per bit increases as we increase the digitization resolution n . This interplay between the digitization resolution n and QCNR is further explored in Fig. 5, where normalized $H_{\min}(M_{\text{dis}}|E)$ is plotted against n for several values of QCNR. We can see that for higher ratios of quantum-to-classical-noise, a lesser amount of digitization resolution is required to achieve a certain value of secure randomness per bit. In other words, even if QCNR cannot be improved further, one can achieve a higher ratio of secure randomness per bit simply by increasing n .

C. Average conditional min-entropy

As described in Section II B, without a bound on the range of classical noise, one cannot extract any secure randomness. However, if we assume that an adversary can only listen to, but has no control over the classical noise, we can estimate the average chance of successful eavesdropping with the *average* guessing probability of M_{dis} given E_{dis} [31, 35, 38],

$$P_{\text{guess}}(M_{\text{dis}}|E_{\text{dis}}) = \left[\sum_{e_j \in E_{\text{dis}}} P_{E_{\text{dis}}}(e_j) \max_{m_i \in M_{\text{dis}}} P_{M_{\text{dis}}|E_{\text{dis}}}(m_i|e_j) \right], \quad (12)$$

Table I. Optimized $\bar{H}_{\min}(M_{\text{dis}}|E)$ (and R) for 8- and 16-bit ADCs

QCNR (dB)	$n = 8$	$n = 16$
∞	7.03 (2.45)	14.36 (3.90)
20	6.93 (2.59)	14.28 (4.09)
10	6.72 (2.93)	14.11 (4.55)
0	6.11 (4.33)	13.57 (6.48)
$-\infty$	0	0

which denotes the probability of correctly predicting the value of discretized measured signal M_{dis} using the optimal strategy, given access to discretized classical noise E_{dis} . Here $P_{E_{\text{dis}}}(e_j)$ is the discretized probability distribution of the classical noise. The extractable secure randomness from our device is then quantified by the average conditional min-entropy

$$\bar{H}_{\min}(M_{\text{dis}}|E_{\text{dis}}) = -\log_2 P_{\text{guess}}(M_{\text{dis}}|E_{\text{dis}}). \quad (13)$$

Here, we again assume that the eavesdropper can measure the full spectrum of the classical noise, with arbitrary precision. This gives the eavesdropper maximum power, including an infinite ADC range $R_e \rightarrow \infty$ and infinitely small binning $\delta_e \rightarrow 0$. As detailed in Appendix B, under these limits, Eq. (13) takes the form of

$$\begin{aligned} \bar{H}_{\min}(M_{\text{dis}}|E) &= \lim_{\delta_e \rightarrow 0} \bar{H}_{\min}(M_{\text{dis}}|E_{\text{dis}}) \\ &= -\log_2 \left[\int_{-\infty}^{\infty} P_E(e) \max_{m_i \in M_{\text{dis}}} P_{M_{\text{dis}}|E}(m_i|e) de \right]. \end{aligned} \quad (14)$$

The full expression of Eq. (14) is shown in Eq. (B7). The optimized result for the average min-entropy $\bar{H}_{\min}(M_{\text{dis}}|E)$ with the corresponding dynamical ADC range R is depicted in Table I. Similar to worst-case min-entropy scenario in Sec. IIB, one can still obtain a significant amount of random bits even if the classical noise is comparable to quantum noise. On the contrary, a conventional unoptimized QNRG requires high operating QCNR to access the high-bitrate regime. When $\text{QCNR} \rightarrow \infty$, the measured signal does not depend on the classical noise and the result coincides with that of the worst-case conditional min-entropy. In fact, the worst-case conditional min-entropy [Eq. (7)] is the lower bound for the average conditional min-entropy [Eq. (13)]. In the absence of side-information E , both entropies will reduce to the usual min-entropy Eq. (5) [31]. Compared to the worst-case min-entropy, the average conditional min-entropy is more robust against degradation of QCNR; hence, it allows one to extract more secure random bits for a given QCNR. This is expected, since in this case, we do not allow the eavesdropper to influence our device, which is a valid assumption for a trusted laboratory.

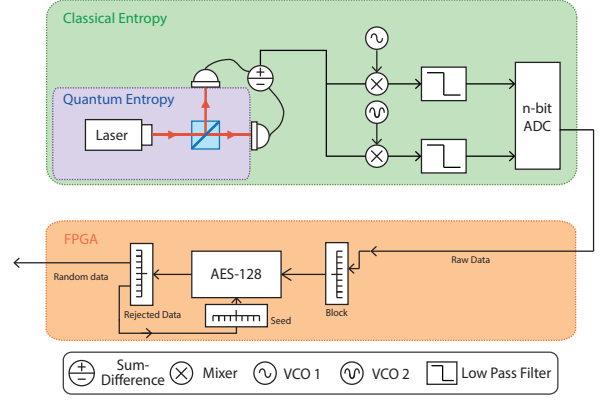


Figure 6. Schematic setup of CVQRNG, where a continuous-variable homodyne detection is performed on the quantum vacuum state, followed by mixing down at 1.375 GHz and 1.625 GHz. The mixing signals are generated by voltage-controlled oscillators. The dynamical ADC range of the ADC is chosen appropriately according to the QCNR and ADC digitization resolution n to maximize the extractable randomness. The raw output, which consists of both quantum and classical contributions, will be postprocessed by field-programmable gate array. A cryptographic hashing function (AES-128) is applied to extract secure randomness quantified by conditional min-entropy.

III. EXPERIMENTAL IMPLEMENTATION

A. Physical setup and characterization

As depicted in Fig. 6, our CVQRNG setup consists of a homodyne detection of the quantum vacuum state followed by post-processing. A 1550-nm fibre-coupled laser (NP Photonic Rock) operating at 60 mW serves as the local oscillator of the homodyning setup. This local oscillator is sent into one port of a 50:50 beam splitter, while the other one is physically blocked and serves as the vacuum input. The outputs are then optically coupled to a pair of balanced photodetectors with 30 dB of common-mode rejection. The intensity of the output ports are recorded over a detection bandwidth of 3 GHz. Since the local oscillator's amplitude α is significantly larger than the quantum vacuum fluctuation, the difference of the photocurrents from the pair of detectors is proportional to $|\alpha| X_v$, where X_v is the quadrature amplitude of the vacuum state. Hence, the contribution of quantum noise is essentially amplified via the balanced homodyne detection.

In order to sample the vacuum field at the spectral range where technical noise is less significant and where the laser is shot-noise limited (see Fig. 7), the electronic output is split and mixed down at 1.375 GHz and 1.625 GHz. Low-pass filters with cutoff frequency at 125 MHz are used to minimize the correlations between the sampling points [40] before digitizing with an appropriately chosen dynamical ADC range parameter R . The measured signal from two sidebands (channel 0, 1.25-1.50

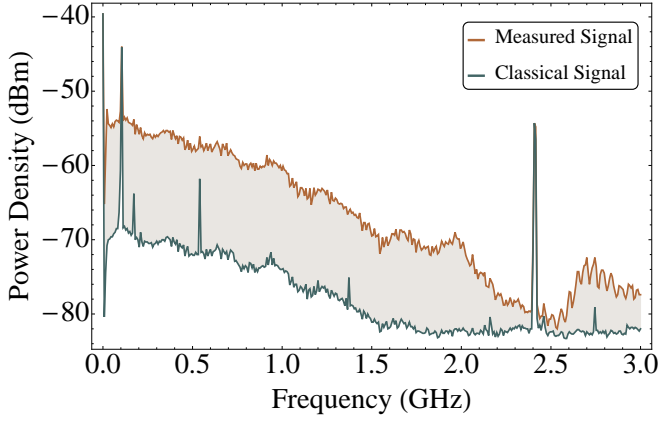


Figure 7. Spectral power density from the CV-QRNG. The measured signal is mixed down at 1.375 GHz and 1.625 GHz (dashed lines), where the laser is shot-noise limited and far from low-frequency technical noise. The QCNr clearances are about 13 dB for both channels, which are sampled at 250 MSamples per second. The shaded region between the measured signal and classical noise indicates the available quantum randomness in our broadband 3-GHz photocurrent detectors, with an average QCNr of approximately 10 dB. The peaks in the classical signal are due to technical noise and pickup signals from radio stations. The peak at 2.4 GHz is due to the Wi-Fi transmissions. The resolution and video bandwidth are both 1 MHz.

GHz), and (channel 1, 1.50-1.75 GHz) are recorded using two 16-bit ADCs (National Instruments 5762) at 250 MSamples per second. Finally, the data processing is performed using a National Instruments field-programmable gate array.

The average QCNr clearances for channel 0 (ch 0) and channel 1 (ch 1) are 13.52 and 13.32 dB, respectively. Taking into account the intrinsic dc offsets, which is $-0.02\sigma_Q$ for both channels, we quantify our conditional min-entropies using the method described in Sec. II. For our ADC with 16 bits of digitization, the worst-case conditional min-entropies are 13.76 bits (ch 0) and 13.75 bits (ch 1), while the average conditional min-entropies are 14.19 bits for both channels. Here, by assuming that the eavesdropper cannot manipulate the classical noise, we evaluate our entropy with average conditional min-entropy and set R as $4.32\sigma_Q$ according to Eq. (B8).

B. Upper bound of extractable min-entropy

The extractable randomness of our QRNG is limited by the sampling rate and the digitization resolution, which is defined by Nyquist's theorem on maximum data rate C ,

$$C = 2H \log_2 V, \quad (15)$$

where H is the bandwidth of the spectrum and $V = 2^n$ is the quantization level for digitization resolution n .

For our 16-bit ADC, the shot-noise-limited and technical-noise-free bandwidth is around 2.5 GHz out of 3 GHz. With an average of 10 dB of QCNr clearance, one can extract 14.11 bits out of 16 bits (Table I). Putting these values into Eq. (15), with a fast enough ADC, we can potentially extract up to 70 Gbit/s random bits out of our detectors.

The maximum bitrate is ultimately upper bounded by the photon number within a given detection time window. In our setup, a 1550-nm fibre-coupled laser with power of 60 mW and detection bandwidth of 3 GHz is used. This corresponds to a mean of 1.6×10^8 photons per sampling. Given a perfect photon-number-resolving detector, the maximum min-entropy is given by $-\log_2(1/\sqrt{2\pi} \times 1.6 \times 10^8) \approx 14.9$ bits (see Appendix C). In principle, one can send more power to extract more random bits, however, this bound can increase only logarithmically with laser intensity.

C. Randomness extraction

It is commonly the case that QRNGs are not ideal sources of randomness, in the sense that the distribution is often biased, while uniform randomness is required for application purposes. In our situation, the quantum vacuum state measured by our CV QRNG exhibits a Gaussian distribution. To generate ideal randomness, post-processing of the raw outputs is necessary to produce shorter, yet almost uniformly distributed random strings. *Ad hoc* algorithms such as the Von Neumann extractor, XOR corrector, and least significant bit operation are widely used [4, 15, 16, 28, 29, 41]. These methods, although simple in practice, might fail to produce randomness at all if non-negligible correlations exist among the raw bits [42].

From an information-theoretic standpoint, universal hashing functions are desirable candidates for randomness extraction [26, 33]. These functions act to recombine bits within a sample according to a randomly chosen seed, and map them to truncated, almost uniform random strings. They constitute a strong extractor which implies that the seed can be reused without sacrificing too much randomness. In recent development of QRNGs [20, 22, 26, 27, 43], they have been used to construct hashing functions such as the Toeplitz-hashing matrix. These constructions require a long (but reusable) seed [44]. A different implementations of an information-theoretic randomness extractor, the Trevisan's extractor, [26, 34, 36] has also received considerable attention. This particular construction of a strong extractor has been proven secure against quantum side-information, and, furthermore, it requires a relatively short seed. Despite so, the complexity of the algorithm imposes a very stringent limit on the extraction speed (0.7 kb/s [26] and 150 kb/s [36]).

Another attractive alternative for secure randomness extraction are cryptographic hashing functions [45–48].

While these cryptographic hashing functions are not information-theoretically proven to be secure, they are still suited for many cryptographic applications and settings where the adversary is assumed to be computationally bounded. The reason for utilizing them over universal hashing functions is that they can have high throughput due to efficient hardware implementation. Previously, cryptographic hashing extractors have been deployed in [11, 13, 18, 24], with functions such as SHA-512 and Whirlpool. Most of the implementations keep exactly min-entropy number of bits, which might not be fully secure (see Appendix D).

Here, we demonstrate randomness extraction with the Advanced Encryption Standard (AES) [49] cryptographic hashing algorithm of 128 bits (see Appendix E). Since a detailed cryptanalysis of our framework is non-trivial and beyond the scope of this paper, we keep only half of our conditional min-entropy [45, 50] to obtain an almost perfectly uniform output. The final real-time guaranteed-secure random number generation rate of our CV QRNG is 3.55 Gbps. If all the available bandwidth from our detector (approximately 2.5 GHz) can be sampled, with sufficient resources, we can achieve up to 35 Gbit/s (cf. Sec. III B). This corresponds to a rate of 14 Mbps/MHz in term of bits per bandwidth. Our random numbers consistently pass the standard statistical tests (NIST [51], DieHard [52]) and the results are available on the Australian National University Quantum Random Number Server (<https://qrng.anu.edu.au>).

IV. CONCLUDING REMARKS

In this work, we propose a generic framework for secure random-number generation, taking into account the existence of classical side information, which, in principle could be manipulated or predicted by an adversary. If the adversary is assumed to have access to the classical noise, for example, the detectors' noise can be originating from preestablished values, the worst-case conditional min-entropy should be used to quantify the available secure randomness. Meanwhile, if we restrict the third party to passive eavesdropping, one can use the average conditional min-entropy instead to quantify extractable randomness. By treating the dynamical ADC range as a free parameter, we show that QCNR is not the sole decisive factor in generating secure random bits. Surprisingly, one can still extract a nonzero amount of secure randomness even when the classical noise is comparable to the quantum noise. This is done simply by optimizing the dynamical ADC range via conditional min-entropies. Such an approach not only provides a rigorous justification for choosing the suitable ADC parameter, but also largely increases the range of QCNR for which true randomness can be extracted, thus relaxing the condition of high QCNR clearance in conventional CV QRNGs. We also notice that we can increase the min-entropy per bit simply by increasing the number of digitization bits. We

apply these observations to analyze the amount of randomness produced by our CV QRNG setup. Efficient cryptographic hashing functions are then deployed to extract randomness quantified by average conditional min-entropy.

We note several possible extensions of our work. For instance, one can apply entropy smoothing [39, 53] on the worst-case min-entropy to tighten the analysis. Our framework can also be generalized to encapsulate potential quantum side information by considering the analysis described in Ref. [27]. A detailed cryptanalysis of our framework can also increase the final throughput of the QRNG [47]. Last, a hybrid of an information-theoretic provable and cryptographic randomness extractor is also an interesting avenue to be explored in the construction of a high-speed, side-information (classical and quantum) proof QRNG [44].

To conclude, this work allows the maximization of extractable high-quality randomness without compromising both the integrity and the speed of a QRNG. In fact, within our framework, when the QRNG is appropriately calibrated, the generated random numbers are secure even if the electronic noise is fully known. This is of practical importance, given the fact that QRNGs play a decisive role in the implementation of cryptographic protocols such as quantum key distribution. From a practical point of view, our method also relaxes the QCNR requirement on the detector, thus allowing QRNGs that are more cost effective and smaller in size. As such, we believe that our work paves the way towards a reliable, high bitrate, and environmentally-immune QRNG [54] for information security.

Note added.— We note several recent papers considering the security aspects of QRNGs [55–58]. A related work by Mitchell *et al.* [59] was published recently. Similar to our work, a lower bound of the average min-entropy was established by assuming the worst-case behavior of various untrusted experimental noise and errors. The study asserts that high-bitrate randomness generation with strong randomness guarantee remains possible even under paranoid analysis, which supports our conclusion.

ACKNOWLEDGEMENT

This research was conducted by the Australian Research Council Centre of Excellence for Quantum Computation and Communication Technology (project number CE110001027). N. N. is funded by the National Research Foundation Competitive Research Programme Space Based Quantum Key Distribution”.

Appendix A: Optimized conditional min-entropy with dc offset

In a realistic scenario, the mean of the measured signal's probability distribution is often nonzero. It is pos-

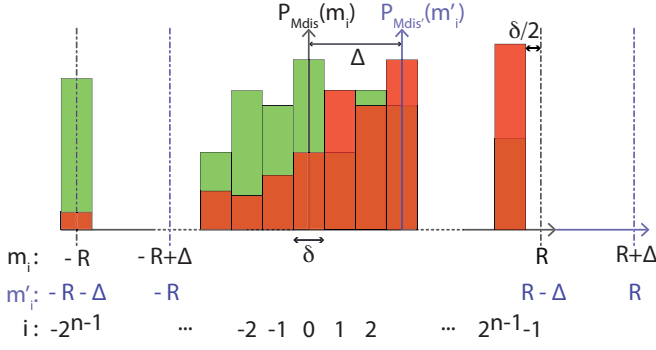


Figure 8. Model of the n -bit ADC, with analog input in the ADC dynamical range $[-R + \delta/2, R - 3\delta/2]$ and bin width $\delta = R/2^{n-1}$. Offset of the distribution is modeled by another reference frame m' centered at offset Δ . In the original frame m , the lowest and highest bins are now centered around $-R - \Delta$ and $R - \delta - \Delta$.

sible that such an offset might be induced by a malicious party over the sampling period. The model is depicted in Fig. 8, where the offset Δ of the distribution is captured by another reference frame m' centered at Δ . In this model, Eq. (4) can now be rewritten as

$$P_{M_{\text{dis}}|E}^{(\Delta)}(m_i|e) = \begin{cases} \int_{-\infty}^{-R-\Delta+\delta/2} p_{M'|E}(m'|e) dm', & i = i_{\min}, \\ \int_{m'_i-\Delta-\delta/2}^{m'_i-\Delta+\delta/2} p_{M'|E}(m'|e) dm', & i_{\min} < i < i_{\max}, \\ \int_{R-3\delta/2-\Delta}^{\infty} p_{M'|E}(m'|e) dm', & i = i_{\max}. \end{cases} \quad (\text{A1})$$

Following the steps in Sec. II and bounding Δ , we finally arrive at the generalization of Eq.(10),

$$H_{\min}(M_{\text{dis}}|E) = -\log_2 \max(c_1, c_2), \quad (\text{A2})$$

Here $c_1 = \frac{1}{2} \left[\text{erf} \left(\frac{e_{\max} + \Delta_{\max} - R + 3\delta/2}{\sqrt{2}} \right) + 1 \right]$ and $c_2 = \text{erf} \left(\frac{\delta}{2\sqrt{2}} \right)$. The results are tabulated in Tables II and III.

Appendix B: Binning of electronic noise - from eavesdropper's perspective

From Eq. (2), the discretized electronic noise distribution on the eavesdropper's ADC with dynamical range R_e and digitization n_e is given by

$$P_{E_{\text{dis}}}(e_j) = \begin{cases} \int_{-\infty}^{-R_e+\delta_e/2} p_E(e) de, & j = j_{\min}, \\ \int_{e_j-\delta_e/2}^{e_j+\delta_e/2} p_E(e) de, & j_{\min} < j < j_{\max}, \\ \int_{R_e-3\delta_e/2}^{\infty} p_E(e) de, & j = j_{\max}, \end{cases} \quad (\text{B1})$$

where $\delta_e = R_e/2^{n_e-1}$ is the corresponding bin width. In order to achieve the lower bound of the average conditional min-entropy described in Eq. (13), we imagine that

the eavesdropper possesses a device with infinite dynamical ADC range and digitization bits, i.e. $R_e \rightarrow \infty$ and $n_e \rightarrow \infty$. As $R_e \rightarrow \infty$, the first and last cases in Eq. (B1) can be discarded, and we are left with

$$P_{E_{\text{dis}}}(e_j) = \int_{e_j-\delta_e/2}^{e_j+\delta_e/2} p_E(e) de. \quad (\text{B2})$$

To evaluate the expression for the discretized conditional probability distribution, we make use of the mean value theorem stated below:

Theorem 1 *Mean value theorem: For any continuous function $f(x)$ on an interval $[a, b]$, there exists some $\bar{x} \in [a, b]$ such that,*

$$\int_a^b f(x) dx = (b-a)f(\bar{x}) \quad (\text{B3})$$

By invoking Theorem 1, there exists $\bar{e}_j \in [e_j - \delta_e/2, e_j + \delta_e/2]$ such that Eq. (B2) can be written as

$$P_{E_{\text{dis}}}(e_j) = p_E(\bar{e}_j)\delta_e. \quad (\text{B4})$$

Substituting this back to Eq. (12), we end up with

$$P_{\text{guess}}(M_{\text{dis}}|E_{\text{dis}}) = \left[\sum_{e_j \in E_{\text{dis}}} p_E(\bar{e}_j)\delta_e \max_{m_i \in M_{\text{dis}}} P_{M_{\text{dis}}|E_{\text{dis}}}(m_i|e_j) \right]. \quad (\text{B5})$$

Assuming an infinite binning $\delta_e \rightarrow 0$, the sum becomes an integral,

$$P_{\text{guess}}(M_{\text{dis}}|E) = \lim_{\delta_e \rightarrow 0} P_{\text{guess}}(M_{\text{dis}}|E_{\text{dis}}) = \left[\int_{-\infty}^{\infty} p_E(e) \max_{m_i \in M_{\text{dis}}} P_{M_{\text{dis}}|E}(m_i|e) de \right]. \quad (\text{B6})$$

Together with Eq. (8), we finally arrive at

$$P_{\text{guess}}(M_{\text{dis}}|E) = \left[\int_{-\infty}^{\infty} p_E(e) \max_{m_i \in M_{\text{dis}}} P_{M_{\text{dis}}|E}(m_i|e) de \right] = \frac{1}{2} \left(\int_{-\infty}^{e_1} P_e(e) \left[1 - \text{erf} \left(\frac{e + R - \delta/2}{\sqrt{2}} \right) \right] de + \left[\text{erf} \left(\frac{e_2}{\sqrt{2}\sigma_E} \right) - \text{erf} \left(\frac{e_1}{\sqrt{2}\sigma_E} \right) \right] \text{erf} \left(\frac{\delta}{2\sqrt{2}} \right) + \int_{e_2}^{\infty} P_e(e) \left[\text{erf} \left(\frac{e - R + 3\delta/2}{\sqrt{2}} \right) + 1 \right] de \right), \quad (\text{B7})$$

where e_1 and e_2 are chosen to satisfy the maximization upon M_{dis} for a given R . The optimal R is then determined numerically. This result can be easily generalized to take into account a dc offset with the steps described

Table II. Optimized $H_{\min}(M_{\text{dis}}|E)$ (and R) for an 8-bit ADC

QCNr (dB)	$ e + \Delta $				
	0	$5\sigma_E$	$10\sigma_E$	$15\sigma_E$	$20\sigma_E$
∞	7.03 (2.45)	7.03 (2.45)	7.03 (2.45)	7.03 (2.45)	7.03 (2.45)
20		6.79 (2.90)	6.58 (3.35)	6.40 (3.81)	6.23 (4.27)
10		6.37 (3.88)	5.91 (5.35)	5.55 (6.85)	5.26 (8.36)
0		5.50 (7.10)	4.75 (11.92)	4.25 (16.82)	3.88 (21.75)
$-\infty$		0	0	0	0

Table III. Optimized $H_{\min}(M_{\text{dis}}|E)$ (and R) for a 16-bit ADC

QCNr (dB)	$ e + \Delta $				
	0	$5\sigma_E$	$10\sigma_E$	$15\sigma_E$	$20\sigma_E$
∞	14.36 (3.90)	14.36 (3.90)	14.36 (3.90)	14.36 (3.90)	14.36 (3.90)
20		14.20 (4.38)	14.05 (4.85)	13.91 (5.33)	13.79 (5.81)
10		13.89 (5.40)	13.53 (6.92)	13.25 (8.46)	13.00 (9.99)
0		13.20 (8.70)	12.56 (13.59)	12.12 (18.51)	11.77 (23.45)
$-\infty$		0	0	0	0

in Appendix A, giving

$$\begin{aligned}
P_{\text{guess}}(M_{\text{dis}}|E) &= \frac{1}{2} \left(\int_{-\infty}^{e_1} p_E(e - \Delta) \left[1 - \text{erf} \left(\frac{e + \Delta + R - \delta/2}{\sqrt{2}} \right) \right] de \right. \\
&+ \left[\text{erf} \left(\frac{e_2 - \Delta}{\sqrt{2}\sigma_E} \right) - \text{erf} \left(\frac{e_1 - \Delta}{\sqrt{2}\sigma_E} \right) \right] \text{erf} \left(\frac{\delta}{2\sqrt{2}} \right) \\
&+ \left. \int_{e_2}^{\infty} p_E(e - \Delta) \left[\text{erf} \left(\frac{e + \Delta - R + 3\delta/2}{\sqrt{2}} \right) + 1 \right] de \right), \quad (\text{B8})
\end{aligned}$$

Appendix C: Upper bound on H_{\min} for limited laser power

For a finite coherent state $|\alpha\rangle$, the maximum value of $H_{\min}(M_{\text{dis}}|E)$ is bounded by the number of photons available in $|\alpha\rangle$. This limit is attained when the ADC discretization is fine enough such that events between n and $n + 1$ photons at the homodyne output can be distinguished (regardless of the amount of classical noise). The probability density function $p_{M|E}(m|e = 0)$ is then a probability mass function having support $(n_1 - n_2)\delta_0$ where n_1 and n_2 are non-negative integers with a Poissonian distribution with mean $|\alpha|^2/2$. The normalization constant $\delta_0 = 1/|\alpha|$ sets the variance to 1. For large $|\alpha|$, the distribution $p_{M|E}(m|e = 0)$ tends to a discretised Gaussian distribution with zero mean and unit variance,

$$P_{M_{\text{dis}}|E}(m|e = 0) = \frac{\delta_0}{\sqrt{2\pi}} \exp(-m^2), \quad (\text{C1})$$

for $m \in \{0, \pm\delta_0, \pm 2\delta_0, \dots\}$. This function has a maximum value of $\delta_0/\sqrt{2\pi}$ at $m = 0$.

For an ADC discretization with bin size δ less than δ_0 and with range large enough such that the probabilities of the two end bins given e , $P_{M_{\text{dis}}|E}(m_{\min}|e)$, and $P_{M_{\text{dis}}|E}(m_{\max}|e)$ are less than $\delta_0/\sqrt{2\pi}$, the most likely bin given e will have a probability of $\delta_0/\sqrt{2\pi}$. The min-entropy of this distribution is then

$$\begin{aligned}
H_{\min}(M_{\text{dis}}|e) &= -\log_2 \left[\max_{m \in M_{\text{dis}}} P_{M_{\text{dis}}|E}(m|e) \right] \\
&= -\log_2 \left(\frac{\delta_0}{\sqrt{2\pi}} \right) \\
&= -\log_2 \left(\frac{1}{\sqrt{2\pi}|\alpha|} \right). \quad (\text{C2})
\end{aligned}$$

Averaging over e , this gives the bound to the average conditional entropy as $\bar{H}_{\min}(M_{\text{dis}}|E) \leq -\log_2(1/\sqrt{2\pi}|\alpha|)$.

Appendix D: Notes on the Leftover Hash Lemma

From an information-theoretic standpoint, the most prominent advantage of universal hashing functions described in Sec. III C is the randomness of the output guaranteed unconditionally by the leftover hash lemma (LHL). More specifically, LHL states that for any $\varepsilon > 0$, if the output of an universal hashing function has length

$$l \leq t - 2 \log_2(1/\varepsilon), \quad (\text{D1})$$

where t denotes the (conditional) min-entropy, then the output will be ε -statistically close to a perfectly uniform distribution [53]. Moreover, a universal hashing function constructs a strong extractor, where the output string is also independent of the seed of the function [26, 33].

On the other hand, for a strong cryptographic extractor, the output is ε' -computationally indistinguishable

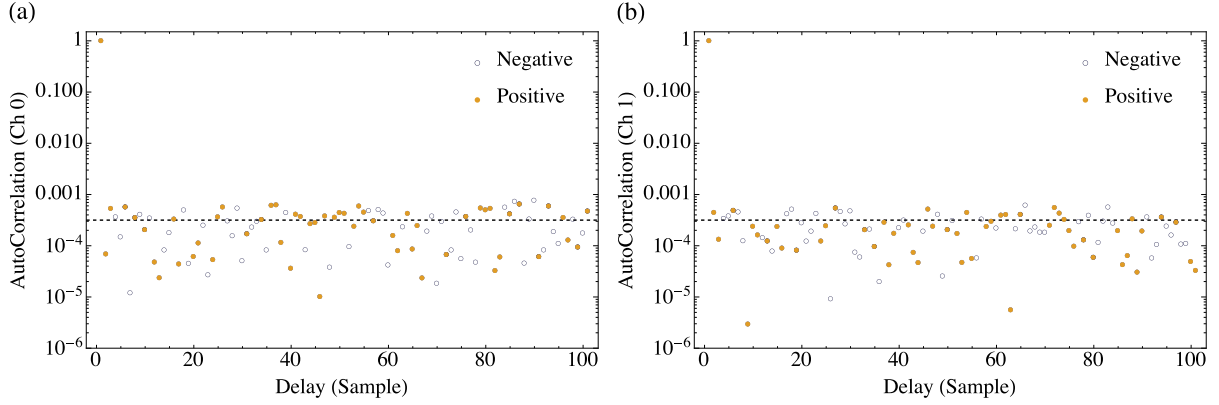


Figure 9. Autocorrelation plots of raw samples for (a) channel 0 and (b) channel 1 evaluated from a typical record of 10^7 consecutive samples. Each sample is 12 bits, where the four most significant bits are discarded from 16-bit raw data. The low values of autocorrelation between the samples are consistent with our raw data being close to independent and identically distributed random variables. Dashed lines show the theoretical standard deviation of truly random 10^7 points.

from the uniform distribution (see Refs. [46, 47] for formal definitions). It is shown in Refs. [48, 53] that LHL can be generalized to take into account almost universal functions (functions statistically ξ -close to being universal hashing functions). This generalized LHL takes the form of $l = \min(t, \log_2(1/\xi)) - 2s$, where s is an integer related to ε' . Under suitable parameter constraints and operating modes, an ε' -cryptographic extractor can be treated as a ξ -almost universal function, and, hence a strong randomness extractor [47, 48]. Hence for a cryptographic extractor, it is necessary to sacrifice some bits according to the desired security parameter ε to ensure the security and uniformity of the output.

Appendix E: AES hashing and auto-correlation

In our QRNG, randomness extraction is performed with an AES [49] cryptographic hashing algorithm of 128 bits seeded with a 128-bit secret initialization vector. Four most significant bits of the 16-bit samples are discarded before randomness extraction to ensure low autocorrelation among consecutive samples (Fig. 9) before hashing. The resulting output is concatenated with partial raw data from the previous run, forming a 128-bit block for cryptographic hashing. Since a complete cryptanalysis of the cryptographic hashing is intricate and is out of the scope of our work, we simply discard half of the output to ensure uniformity of the generated random sequence [50]. We further strengthen our security by renewing the seed of our AES extractor with these discarded bits. The final real-time throughput of our CV QRNG is 3.55 Gbits/s.

-
- [1] Mario Stipčević, “Quantum random number generators and their use in cryptography,” in *Proceedings of 34th International Convention MIPRO* 1474-1479 (2011).
 - [2] P Xu, YL Wong, TK Horiuchi, and PA Abshire, “Compact floating-gate true random number generator,” *Electronics Letters* **42**, 1346–1347 (2006).
 - [3] Berk Sunar, William J Martin, and Douglas R Stinson, “A provably secure true random number generator with built-in tolerance to active attacks,” *Computers, IEEE Transactions on* **56**, 109–119 (2007).
 - [4] Atsushi Uchida, Kazuya Amano, Masaki Inoue, Kunihito Hirano, Sunao Naito, Hiroyuki Someya, Isao Oowada, Takayuki Kurashige, Masaru Shiki, Shigeru Yoshimori, et al., “Fast physical random bit generation with chaotic semiconductor lasers,” *Nature Photonics* **2**, 728–732 (2008).
 - [5] Ido Kanter, Yaara Aviad, Igor Reidler, Elad Cohen, and Michael Rosenbluh, “An optical ultrafast random bit generator,” *Nature Photonics* **4**, 58–61 (2010).
 - [6] Davide G Marangon, Giuseppe Vallone, and Paolo Villoresi, “Random bits, true and unbiased, from atmospheric turbulence,” *Scientific reports* **4** (2014).
 - [7] Cristian S Calude, Michael J Dinneen, Monica Dumitrescu, and Karl Svozil, “Experimental evidence of quantum randomness incomputability,” *Physical Review A* **82**, 022102 (2010).
 - [8] Karl Svozil, “Three criteria for quantum random-number generators based on beam splitters,” *Physical Review A* **79**, 054306 (2009).
 - [9] Bing Qi, Yue-Meng Chi, Hoi-Kwong Lo, and Li Qian, “High-speed quantum random number generation by measuring phase noise of a single-mode laser,” *Optics Letters* **35**, 312–314 (2010).

- [10] Hong Guo, Wenzhuo Tang, Yu Liu, and Wei Wei, “Truly random number generation based on measurement of phase noise of a laser,” *Physical Review E* **81**, 051137 (2010).
- [11] M Jofre, M Curty, F Steinlechner, G Anzolin, JP Torres, MW Mitchell, and V Pruneri, “True random numbers from amplified quantum vacuum,” *Optics Express* **19**, 20665–20672 (2011).
- [12] Feihu Xu, Bing Qi, Xiongfeng Ma, He Xu, Haoxuan Zheng, and Hoi-Kwong Lo, “Ultrafast quantum random number generation based on quantum phase fluctuations,” *Optics Express* **20**, 12366–12377 (2012).
- [13] C Abellán, W Amaya, M Jofre, M Curty, A Acín, J Capmany, V Pruneri, and MW Mitchell, “Ultra-fast quantum randomness generation by accelerated phase diffusion in a pulsed laser diode,” *Optics Express* **22**, 1645–1654 (2014).
- [14] Mario Stipčević and B Medved Rogina, “Quantum random number generator based on photonic emission in semiconductors,” *Review of scientific instruments* **78**, 045104 (2007).
- [15] Caitlin RS Williams, Julia C Salevan, Xiaowen Li, Rajarshi Roy, and Thomas E Murphy, “Fast physical random number generator using amplified spontaneous emission,” *Optics Express* **18**, 23584–23597 (2010).
- [16] Y Liu, MY Zhu, B Luo, JW Zhang, and H Guo, “Implementation of 1.6 tb s⁻¹ truly random number generation based on a super-luminescent emitting diode,” *Laser Physics Letters* **10**, 045001 (2013).
- [17] Michael Wahl, Matthias Leifgen, Michael Berlin, Tino Röhlicke, Hans-Jürgen Rahn, and Oliver Benson, “An ultrafast quantum random number generator with provably bounded output bias based on photon arrival time measurements,” *Applied Physics Letters* **98**, 171105 (2011).
- [18] Michael A Wayne and Paul G Kwiat, “Low-bias high-speed quantum random number generator via shaped optical pulses,” *Optics Express* **18**, 9351–9357 (2010).
- [19] Hai-Qiang Ma, Yuejian Xie, and Ling-An Wu, “Random number generation based on the time of arrival of single photons,” *Appl. Opt.* **44**, 7760–7763 (2005).
- [20] Philip J Bustard, Duncan G England, Josh Nunn, Doug Moffatt, Michael Spanner, Rune Lausten, and Benjamin J Sussman, “Quantum random bit generation using energy fluctuations in stimulated raman scattering,” *Optics Express* **21**, 29350–29357 (2013).
- [21] M Fiorentino, C Santori, SM Spillane, RG Beausoleil, and WJ Munro, “Secure self-calibrating quantum random-bit generator,” *Physical Review A* **75**, 032334 (2007).
- [22] Giuseppe Vallone, Davide G Marangon, Marco Tomasin, and Paolo Villoresi, “Quantum randomness certified by the uncertainty principle,” *Physical Review A* **90**, 052327 (2014).
- [23] Thomas Symul, SM Assad, and Ping K Lam, “Real time demonstration of high bitrate quantum random number generation with coherent laser light,” *Applied Physics Letters* **98**, 231103 (2011).
- [24] Christian Gabriel, Christoffer Wittmann, Denis Sych, Ruifang Dong, Wolfgang Mauere, Ulrik L Andersen, Christoph Marquardt, and Gerd Leuchs, “A generator for unique quantum random numbers based on vacuum states,” *Nature Photonics* **4**, 711–715 (2010).
- [25] Bruno Sanguinetti, Anthony Martin, Hugo Zbinden, and Nicolas Gisin, “Quantum random number generation on a mobile phone,” *Phys. Rev. X* **4**, 031056 (2014).
- [26] Xiongfeng Ma, Feihu Xu, He Xu, Xiaoqing Tan, Bing Qi, and Hoi-Kwong Lo, “Postprocessing for quantum random-number generators: Entropy evaluation and randomness extraction,” *Physical Review A* **87**, 062327 (2013).
- [27] Daniela Frauchiger, Renato Renner, and Matthias Troyer, “True randomness from realistic quantum devices,” *arXiv preprint arXiv:1311.4547* (2013).
- [28] Neus Oliver, Miguel Cornelles Soriano, David W. Sukow, and Ingo Fischer, “Fast Random Bit Generation Using a Chaotic Laser: Approaching the Information Theoretic Limit,” *IEEE Journal of Quantum Electronics* **49**, 910–918 (2013).
- [29] T. Yamazaki and A. Uchida, “Performance of Random Number Generators Using Noise-Based Superluminescent Diode and Chaos-Based Semiconductor Lasers,” *IEEE Journal of Selected Topics in Quantum Electronics* **19**, 060030 (2013).
- [30] S Pironio, A Acín, and S Massar, “Random numbers certified by Bell’s theorem,” *Nature* **464**, 1021–1024 (2010).
- [31] Stefano Pironio and Serge Massar, “Security of practical private randomness generation,” *Physical Review A* **87**, 012336 (2013).
- [32] BG Christensen, KT McCusker, JB Altepeter, B Calkins, T Gerrits, AE Lita, A Miller, LK Shalm, Y Zhang, SW Nam, et al., “Detection-loop-hole-free test of quantum nonlocality, and applications,” *Physical Review Letters* **111**, 130406 (2013).
- [33] Ronen Shaltiel, “Recent developments in explicit constructions of extractors,” *Bulletin of the EATCS* **77**, 67–95 (2002).
- [34] Anindya De, Christopher Portmann, Thomas Vidick, and Renato Renner, “Trevisan’s extractor in the presence of quantum side information,” *SIAM Journal on Computing* **41**, 915–940 (2012).
- [35] R König, Renato Renner, and Christian Schaffner, “The operational meaning of min-and max-entropy,” *Information Theory, IEEE Transactions on* **55**, 4337–4347 (2009).
- [36] Wolfgang Mauere, Christopher Portmann, and Volkher B Scholz, “A modular framework for randomness extraction based on trevisan’s construction,” *arXiv preprint arXiv:1212.0520* (2012).
- [37] Yun Zhi Law, Jean-Daniel Bancal, Valerio Scarani, et al., “Quantum randomness extraction for various levels of characterization of the devices,” *Journal of Physics A: Mathematical and Theoretical* **47**, 424028 (2014).
- [38] Yevgeniy Dodis, Rafail Ostrovsky, Leonid Reyzin, and Adam Smith, “Fuzzy extractors: How to generate strong keys from biometrics and other noisy data,” *SIAM Journal on Computing* **38**, 97–139 (2008).
- [39] Renato Renner, “Security of quantum key distribution,” *International Journal of Quantum Information* **6**, 1–127 (2008).
- [40] Yong Shen, Liang Tian, and Hongxin Zou, “Practical quantum random number generator based on measuring the shot noise of vacuum states,” *Physical Review A* **81**, 063814 (2010).
- [41] Thomas Durt, Carlos Belmonte, Louis-Philippe Lamoureux, Krassimir Panajotov, Frederik Van den Berghe, and Hugo Thienpont, “Fast quantum-optical random-number generators,” *Physical Review A* **87**, 022339 (2013).

- (2013).
- [42] Boaz Barak, Ronen Shaltiel, and Eran Tromer, “True random number generators secure in a changing environment,” Cryptographic Hardware and Embedded Systems - CHES 2003, 166–180 (2003).
 - [43] You-Qi Nie, Hong-Fei Zhang, Zhen Zhang, Jian Wang, Xiongfeng Ma, Jun Zhang, and Jian-Wei Pan, “Practical and fast quantum random number generation based on photon arrival time relative to external reference,” Applied Physics Letters **104**, 051110 (2014).
 - [44] Boaz Barak, Yevgeniy Dodis, Hugo Krawczyk, Olivier Pereira, Krzysztof Pietrzak, François-Xavier Standaert, and Yu Yu, “Leftover hash lemma, revisited,” in Advances in Cryptology–CRYPTO 2011 (Springer, 2011) pp. 1–20.
 - [45] Yevgeniy Dodis, Rosario Gennaro, Johan Håstad, Hugo Krawczyk, and Tal Rabin, “Randomness extraction and key derivation using the cbc, cascade and hmac modes,” in Advances in Cryptology–CRYPTO 2004 (Springer, 2004) pp. 494–510.
 - [46] Hugo Krawczyk, “Cryptographic extraction and key derivation: The hkdf scheme,” in Advances in Cryptology–CRYPTO 2010 (Springer, 2010) pp. 631–648.
 - [47] Yvonne Cliff, Colin Boyd, and Juan Gonzalez Nieto, “How to extract and expand randomness: A summary and explanation of existing results,” in Applied Cryptography and Network Security (Springer, 2009) pp. 53–70.
 - [48] Olivier Chevassut, Pierre-Alain Fouque, Pier-ric Gaudry, and David Pointcheval, “The twist-augmented technique for key exchange,” in Public Key Cryptography-PKC 2006 (Springer, 2006) pp. 410–426.
 - [49] PUB FIPS, “197: Advanced encryption standard (aes),” National Institute of Standards and Technology (2001).
 - [50] Elaine Barker and John Kelsey, “Recommendation for the entropy sources used for random bit generation,” NIST DRAFT Special Publication 800-90B (2012).
 - [51] Andrew Rukhin, Juan Soto, James Nechvatal, Elaine Barker, Stefan Leigh, Mark Levenson, David Banks, Alan Heckert, James Dray, San Vo, et al., “Statistical test suite for random and pseudorandom number generators for cryptographic applications, nist special publication,” (2010).
 - [52] Georges Marsaglia, “Diehard test suite,” Online: <http://www.stat.fsu.edu/pub/diehard/>. Last visited 8, 2014 (1998).
 - [53] Marco Tomamichel, Christian Schaffner, Adam Smith, and Renato Renner, “Leftover hashing against quantum side information,” Information Theory, IEEE Transactions on **57**, 5524–5535 (2011).
 - [54] Nicolas Gisin and Robert Thomas Thew, “Quantum communication technology,” Electronics letters **46**, 965–967 (2010).
 - [55] Pavel Pavel Lougovski and Raphael Pooser, “An observed-data-consistent approach to the assignment of bit values in a quantum random number generator,” arXiv preprint arXiv:1404.5977 (2014).
 - [56] Mario Stipčević and John Bowers, “Post-processing free spatio-temporal optical random number generator resilient to hardware failure and signal injection attacks,” arXiv preprint arXiv:1410.0724 (2014).
 - [57] Tommaso Lunghi, Jonatan Bohr Brask, Charles Ci Wen Lim, Quentin Lavigne, Joseph Bowles, Anthony Martin, Hugo Zbinden, and Nicolas Brunner, “Self-Testing Quantum Random Number Generator,” Physical Review Letters **114**, 150501 (2015).
 - [58] Gustavo Cañas, Jaime Cariñe, Esteban S Gómez, Johanna F Barra, Adán Cabello, Guilherme B Xavier, Gustavo Lima, and Marcin Pawłowski, “Experimental quantum randomness extraction invulnerable to detection loophole attacks,” arXiv preprint arXiv:1410.3443 (2014).
 - [59] Morgan W. Mitchell, Carlos Abellan, and Waldimar Amaya, “Strong experimental guarantees in ultrafast quantum random number generation,” Phys. Rev. A **91**, 012314 (2015).